



Published in final edited form as:

Muscle Nerve. 2017 September ; 56(3): 486–494. doi:10.1002/mus.25503.

SEVERE MURINE LIMB-GIRDLE MUSCULAR DYSTROPHY TYPE 2C PATHOLOGY IS DIMINISHED BY FTY720 TREATMENT

Ahlke Heydemann, PhD^{1,2}

¹Department of Physiology and Biophysics, University of Illinois at Chicago, 835 South Wolcott Avenue, COMRB 2035, MC 901, Chicago, Illinois 60612, USA

²The Center for Cardiovascular Research, University of Illinois at Chicago, Chicago, Illinois, USA

Abstract

Introduction—Limb-girdle muscular dystrophy type 2C (LGMD-2C) is caused by mutations in γ -sarcoglycan and is a devastating, progressive, and fully lethal human muscle-wasting disease that has no effective treatment. This study examined the efficacy of the sphingosine-1-phosphate receptor modulator FTY720 in treating *Sgcg*^{-/-} DBA2/J, a severe mouse model of LGMD-2C. FTY720 treatment was expected to target LGMD-2C disease progression at 2 key positions by reducing chronic inflammation and fibrosis.

Methods—The treatment protocol was initiated at age 3 weeks and was continued with alternate-day injections for 3 weeks.

Results—The treatment produced significant functional benefit by plethysmography and significant reductions of membrane permeability and fibrosis. Furthermore, the protocol elevated protein levels of δ -sarcoglycan, a dystrophin–glycoprotein family member.

Conclusion—This study showed that FTY720 is an effective muscular dystrophy treatment when therapy is initiated early in the disease progression.

Keywords

fibrosis; dystrophin–glycoprotein complex; FTY720; mouse model; muscular dystrophy; sphingosine-1-phosphate

Mutations in γ -sarcoglycan cause limb-girdle muscular dystrophy type 2C (LGMD-2C) in humans, and *Sgcg*^{-/-} in mice. In both species, the disease progresses along an overlapping series of events.¹ The initial insult is membrane tears and increased permeability due to the lack of an essential structural protein. The increased permeability initiates a series of pathologic events, including chronic inflammation, increased serum creatine kinase, increased Evans blue dye uptake, and dysregulation of calcium and multiple other signaling molecules. These events lead to myofiber degeneration and regeneration and eventual inability to replace the myofibers due to a weakened and decreased satellite cell pool. The myofibers are replaced with myofibroblasts and fibroblasts, which deposit excessive

Correspondence to: A. Heydemann; ahlkeh@uic.edu.

Additional Supporting Information may be found in the online version of this article.

extracellular matrix (ECM). In normal skeletal muscle wound-healing, the satellite cell pool is maintained, and the ECM is remodeled to decrease the size of the scar, if any remains. In muscular dystrophy (MD), the satellite cells are impeded by chronic inflammation,² excessive fibrosis, and excessive ECM,³ and the muscles are incapable of remodeling the scar tissue at the required pace.

Multiple genes can be mutated to cause human and murine MD.⁴ Most common are mutations in the dystrophin gene, specifically those causing Duchenne MD (DMD) in humans and modeled by the *mdx* mouse. Another member of the dystrophin–glycoprotein complex (DGC), γ -sarcoglycan, is mutated in humans and causes limb-girdle MD type 2C and, through genetic engineering, a mouse line with a targeted allele of γ -sarcoglycan has been generated (signified by *Sgcg*; see Hack *et al.*⁵). The *Sgcg* mutation has been established in multiple mouse strains,⁶ and the null mutation on the DBA2/J (*Sgcg*^{-/-}D2) mouse strain was identified as the most severely affected.^{6,7} The *Sgcg*^{-/-}D2 mice were more severely affected than *mdx* mice on their usual C57/B110 strain.¹ Therefore, for this work, I used *Sgcg*^{-/-}D2 mice to robustly test the ability of FTY720 to inhibit disease progression.

Currently, there are no effective treatments for DMD or LGMD.⁸ The current standard of care is corticosteroids, which are believed to function through immune inhibition. However, these compounds produce many unwanted side effects when taken on a long-term basis.⁹ Therefore, these experiments were initiated to identify the potential of FTY720 to inhibit LGMD disease progression. FTY720 (Fingolimod or Gilyena; Novartis) has been approved by the Food and Drug Administration to treat relapsing–remitting multiple sclerosis; it significantly reduces the rate of relapses.¹⁰ FTY720 is a sphingosine-1-phosphate receptor modulator, which acts by reducing chronic inflammation.¹¹ In a mouse model of pressure overload cardiac disease, FTY720-P has proven beneficial in reducing fibrosis through the serine/threonine–protein kinase (PAK1) signaling cascades.¹² The evidence for PAK1 dependence has been generated by utilizing PAK1 cardiac-specific knockout mice and PAK1 siRNA technology¹³; in both cases, FTY720 treatment becomes ineffective without PAK1.

The S1P signaling cascade is truly complex and beyond the scope of this study. However, S1P signaling is impacted by concentration, concentration gradients, responding cell history (receptors and the associated heterotrimeric G proteins coupled to them), rate of phosphorylation and dephosphorylation, and rate of S1P degradation (all very well reviewed elsewhere¹⁴). S1P signaling is also known to modulate many cellular processes. Specifically, in muscle cells, S1P signaling modulates immune function, decreases HDAC1 and HDAC2 activities,¹⁵ promotes satellite cell proliferation and differentiation, increases satellite cell response to cardiotoxin, and increases myofiber size.¹⁶ There are many reports of immune inhibition, including corticosteroids, aiding MD patients and animal models.¹⁷ Many of the other S1P cellular effects listed above are also hypothesized to reduce MD phenotypes.

S1P signaling can be beneficially increased genetically, biochemically, and pharmacologically.¹⁸ Increasing S1P signaling benefits *Drosophila* with MD, as observed by reducing the well-documented wing vein defect and increasing movement. Furthermore, treating cardiotoxin acutely injured *mdx* mice with THI (a small-molecule S1P lyase inhibitor) increases S1P and increases muscle integrity and function. Studies have identified

that treating uninjured 4-week-old *mdx* mice with TH1 for 4 weeks increased the *ex-vivo* maximum force created by the extensor digitorum longus.

Despite this robust investigation into S1P signaling, quantifying phenotypic changes in uninjured dystrophic murine muscles by pharmaceutically increasing S1P has not been done. This study investigated the effectiveness of FTY720 to reduce LGMD-2C mediated pathology.

METHODS

The *Sgcg*^{+/-} mice on the DBA2/J (*Sgcg*^{+/-}D2) background were generously provided by Dr. Elizabeth McNally.^{5,6} The mice were maintained in a barrier facility with 12-hour light/dark cycles and received standard lab chow and water *ad libitum*. All animal protocols adhered to the *Guide for the Care and Use of Laboratory Animals* (National Institutes of Health) and the protocol of the institutional animal care and use committee of the University of Illinois at Chicago. The *Sgcg*^{-/-} mice were randomly assigned to the prevention group (start at age 3 weeks, before fibrosis has begun, and treat for 3 weeks) or the reversal group (start at age 10 weeks, near the peak of fibrosis,¹ and treat for 3 weeks) and also randomly assigned to receive FTY720 (Cayman Chemicals, Ann Arbor, Michigan) at 10µg/g or vehicle intraperitoneally every other day (Fig. 1). The FTY720 was first dissolved in dimethylsulfoxide (DMSO) to 100µg/µl. It was diluted 1:50 in 0.9% sodium chloride before 5 µl/g body weight injection, and the vehicle animals received DMSO diluted 1:50 in 0.9% sodium chloride at 5 µl/g body weight injection.

Before harvest, I performed plethysmography and echocardiography to assess functional components of the expected fibrosis reduction by FTY720. Plethysmography was done on a small-animal whole-body device (Buxco/DSI, St. Paul, Minnesota) with Finepointe software (Buxco) for analysis. As described previously, the mice were acclimatized in the chambers for 10 minutes before respiratory values were recorded for 15 minutes. The animals were then sequentially placed in the next 3 chambers for a total of 60 minutes of recordings. If all chambers provided very similar values (averages within each other's standard deviations), all 60 minutes of recordings were averaged and used for analysis. Rarely, 1 chamber would give aberrant results, and its data would be disregarded. Echocardiography and analysis were performed by Robert Gaffin on a digital imaging system (Vevo 2100; Visualsonics, Toronto, Ontario, Canada) at the University of Illinois at Chicago Center for Cardiovascular Research.

Forty hours before harvest the mice were injected with Evans blue dye (EBD; Sigma Aldrich, St. Louis, Missouri; Sigma was the source of all chemicals) 10 mg/ml diluted in phosphate-buffered saline (PBS) at a final ratio of 5 µl/g of animal weight. Forty hours of EBD was previously determined empirically to minimize background EBD in wild-type mice.⁶ The animals were euthanized with carbon dioxide, followed by cervical dislocation. Multiple muscle tissues were harvested, minced, weighed in microcentrifuge tubes, and frozen at -80°C for EBD uptake quantification (abdominal muscles 1 × 1-cm² segment, half of each quadriceps, both gastrocnemius/soleus, half of each gluteus, triceps, and kidneys as EBD injection controls, for a total of 11 tissues) or hydroxyproline (HOP) quantification

(abdominal muscles $1 \times 1\text{-cm}^2$ segment, diaphragm, cardiac ventricles, half of each quadriceps, half of each gluteus, for a total of 9 tissues). Some muscle tissues (center quadriceps slice, tibialis anterior, and the heart base) were harvested for histology and immunofluorescence by submerging the pieces in optimal cutting temperature medium (Tissue-Tek, Sakura Finetek, Torrance, California) and freezing in liquid nitrogen-cooled isopentane. In addition, center disks from the quadriceps were placed in neutral-buffered formalin for histologic processing. The veterinary clinic at the University of Illinois at Champaign processed the tissues and performed Masson trichrome staining.

Membrane permeability was quantified utilizing a high-throughput assay that uses spectrophotometry to quantify EBD eluted from tissue.⁶ The microcentrifuge tubes containing the weighed frozen tissues received 500 μl of formamide and were vortexed and incubated at 55°C for at least 2 hours. Two hundred microliters of the resulting elution was transferred into a 96-well plate, and the optical density was measured at 580\AA . A standard curve was also generated; the values are reported as $\text{mM EBD}/\mu\text{g}$ tissue. The muscle EBD uptake values were then divided by the animal's average kidney EBD uptake to normalize for injection quality and to normalize for the effects of FTY720 upon blood vessel permeability.

The HOP assay was used to quantify the collagen content of various muscles as a reflection of the fibrosis present.⁶ The microcentrifuge tubes containing the HOP samples received 500 μl of 6 M HCl, were vortexed, and incubated at 105°C overnight. Ten microliters of the hydroxylate was moved to another microcentrifuge tube, which received 150 μl of isopropanol followed by 75 μl of chloramine T (7% solution in water) mixed 1:4 with citrate acetate buffer (1.44M sodium acetate, 5.75 M citric acid, 0.435M NaOH, 3.85% of isopropanol in water). The mixture was vortexed and incubated at room temperature for 10 minutes. Then, 1ml of Ehrlich reagent (0.3% *p*-dimethylaminobenzaldehyde in ethanol with 6.75% sulfuric acid) diluted 3:13 in isopropanol was added. This mixture was incubated for 30 minutes at 58°C , the reaction was quenched on ice for 5 minutes before a quick centrifugation and reading 200 μl on a 96-well plate at $620/\text{\AA}$. A standard curve with hydroxyproline was generated. The results are reported as $\text{mM HOP}/\mu\text{g}$ tissue.

Immunofluorescence was performed on $10\text{-}\mu\text{m}$ frozen quadriceps sections. Sections from all animal groups were affixed to a single slide for each stain to minimize staining artifacts. The tissue sections were fixed in methanol at -20°C for 5 minutes, followed by PBS rinses and non-specific epitope blocking in 5% fetal bovine serum in $1 \times \text{PBS}$ for 20 minutes at room temperature. Primary antibodies fibronectin and δ -sarcoglycan (both from Santa Cruz Biotechnology, Santa Cruz, California) were diluted 1:100 in blocking solution and incubated on the slides in a wet chamber overnight at 4°C . After 3 15-minute $1 \times \text{PBS}$ washes at room temperature, appropriate species-specific secondary antibodies (Invitrogen, Waltham, Massachusetts) diluted 1:2,500 in blocking solution were applied for 1 hour at room temperature. After a final set of 3 15-minute $1 \times \text{PBS}$ washes at room temperature, the coverslips were mounted with DAPI Vectashield media (Vector Labs, Burlingame, California). Images were acquired on a photomicroscope (Zeiss Axio-photo; Carl Zeiss, Jena, Germany) at $20\times$ original magnification. Representative images are shown.

One-way analyses of variance (ANOVAs) with a *post-hoc* Tukey test were calculated with StatView software, and $P < 0.05$ were considered significant.

RESULTS

Preliminary analysis of a small cohort (12 animals) from the reversal strategy indicated no benefit (data not shown). Therefore, all data presented here are from the prevention cohort.

Gross Anatomy

At harvest time, pictures of the *Sgcg*^{-/-}D2-treated and untreated diaphragms and hearts were obtained (representative images shown in Fig. 2). In the diaphragms, the FTY720 treatment clearly reduced EBD staining and fibrotic scars. Figure 2A shows a dystrophic diaphragm from an animal receiving the diluted DMSO vehicle; the blue rays indicate permeable membrane, and therefore EBD-penetrated myofibers. Figure 2B is a representative image of diaphragm from a dystrophic littermate that received FTY720 for 3 weeks. The EBD intensity is much weaker, and fewer fibers have any blue at all.

The representative FTY720-treated heart also displays decreased gross pathology compared with the DMSO-treated littermate. Although the hearts are dark, EBD uptake differences can be grossly determined by a more intensely darker blue in the vehicle heart (Fig. 2C) compared with the less-intense blue of the FTY720-treated heart (Fig. 2D). In addition, there was a significant reduction in gross fibrosis in cardiac fibers after 3 weeks of FTY720 treatment. The control-treated heart shows a right ventricle that is very fibrotic, and the representative FTY720 treated heart has less fibrosis in the right ventricle (Fig. 2C and D).

Membrane Permeability

Using a quantifiable EBD uptake assay,⁶ I found that FTY720 treatment reduced membrane permeability in all skeletal muscle tissues analyzed, except for the abdominal muscles (see Fig. 3A for averages and standard errors, and Table 1). FTY720 treatment also reduced EBD uptake into the wild-type muscles (Fig. 3A). Multiple publications have demonstrated that increasing S1P signaling decreases endothelial barrier penetrance.²⁰ Therefore, we normalized the EBD skeletal muscle uptake values by the kidney EBD uptake values (Fig. 3B and Table 1). The kidneys were originally harvested and quantified to control for the intraperitoneal injection (IP) EBD injections. When skeletal muscle EBD uptake values were normalized to kidney EBD uptake values, a significant benefit of FTY720 treatment was still observed in LGMD mice, again with the exception of abdominal muscles.

I used immunofluorescent staining for another member of the DGC on quadriceps muscle tissue sections from the 4 prevention mouse groups. When γ -sarcoglycan is absent in patients or in the murine model of LGMD-2C, other DGC members are reduced.^{5,21} In the FTY720-treated dystrophic muscles, enhanced immunofluorescent staining of δ -sarcoglycan was seen (representative pictures in Fig. 4). FTY720 treatment also increased δ -sarcoglycan staining in the quadriceps of the wild-type mice. A schematic of the 2 mechanisms in which FTY720 reduces EBD uptake into muscle tissue is shown in Figure 4.

Fibrosis Assessment

I also analyzed the fibrosis content of various muscle groups with a quantitative HOP assay.⁶ The prevention protocol significantly reduced fibrosis in all muscle groups tested, including the clinically important cardiac ventricles and diaphragm (Fig. 5 and Table 1). FTY720 treatment did not produce any significant fibrotic changes in the wild-type mice. To confirm this fibrotic reduction, immunofluorescence for fibronectin was performed in quadriceps muscles. In support of the quantitative assay, immunofluorescence demonstrated that FTY720 treatment reduced fibronectin, and therefore fibrosis (Fig. 5). Masson trichrome staining also indicated fibrosis reduction after 3 weeks of FTY720 treatment (Fig. 5). This stain also identifies decreased immune cell infiltrate after FTY720 treatment. Because it has been postulated that LGMD-mediated fibrosis causes the functional decline of the muscles, I next tested various functional characteristics of the diaphragm and cardiac muscles.

Plethysmography

Whole-body plethysmography can identify diaphragm fibrosis through decreased peak inhalation flow (PIF), peak exhalation flow (PEF), minute volume (MV), and velocity at 50% exhalation volume (EF₅₀). The vehicle-treated *Sgcg*^{-/-}D2 mice had significantly decreased PIF, PEF, MV, and EF₅₀ compared with the wild-type D2 mice, indicating functional reduction as early as 6 weeks in this LGMD-2C model (Fig. 6).

Echocardiography

I also performed echocardiography on the 4 mouse groups from the prevention protocol to analyze their cardiac functional changes. No significant changes were observed.

DISCUSSION

This study has shown that 3 weeks of alternate-day FTY720 treatment can prevent but cannot reverse disease phenotypes in a severe mouse model of LGMD-2C. I have established that 10µg/g of animal body weight delivered intraperitoneally (IP) every other day starting at age 3 weeks reduces sarcolemmal permeability, reduces muscle fibrosis, and increases function of muscles from a *Sgcg*^{-/-} mouse model of LGMD-2C.

I aimed to determine efficacy for FTY720 use in murine MD. I initiated these experiments with the prevention strategy of injections (10 µg/g) starting at age 3 weeks and continuing every day for 3 weeks. The FTY720 recipient animals weighed significantly less than the vehicle animals after just 1 week of injections (FTY720: 7.8 ± 0.43 g; vehicle: 8.9 ± 0.12 g; *P* = 0.04). Furthermore, at the 2-week injection time-point, the FTY720 animals demonstrated lethargy and unkempt fur. The treated and control animals were promptly harvested, and the FTY720-treated group demonstrated decreased HOP (data not shown). Based on these preliminary data, experiments continued, but subsequent animals received the same dose of FTY720 (10 µg/g) every other day. The prevention strategy initiated IP injections at age 3 weeks and continued every other day for 3 weeks. The reversal strategy started IP injections at age 10 weeks and continued every other day for 3 weeks. The reversal strategy did not demonstrate any benefit by gross visualization, histology, EBD uptake, HOP content, plethysmography, or echocardiography. Therefore, all of the results

are from the prevention animal groups. EBD is known to bind albumin,²² which then penetrates into cells with damaged and permeable membranes. Scientists have used EBD cell penetrance as an indicator of permeable cell membranes due to the lack of an intact DGC.²³ I believe that the reduced EBD in the FTY720-treated *Sgcg*^{-/-}D2 mice result from 2 mechanisms (modeled in Fig. 4). A portion of the reduction arises from the reduced endothelial cell permeability known to be caused by S1P signaling²⁴ and FTY720 signaling.²⁵ I make this statement, because, when the skeletal muscle EBD uptake values were normalized to the animal's kidney EBD values, the differences between the 2 *Sgcg*^{-/-}D2 mouse groups decreased, but it remained significant. Furthermore, the treated and untreated wild-type muscle groups were no longer significantly different after kidney normalization. The remainder of the difference between the 2 *Sgcg*^{-/-} mouse groups arose from FTY720's beneficial effects on membrane integrity. Reduced membrane permeability is also evident from the representative diaphragm images of Figure 2. Not only was there less blue in the damaged fibers (indicative of reduced endothelial cell permeability), but there were also fewer blue fibers (indicative of fewer fibers with damaged sarcolemmas). Enhanced membrane strength can also be surmised from the reappearance of δ -sarcoglycan in the sarcolemma by immunofluorescence (Fig. 4). Interestingly, FTY720 treatment increased δ -sarcoglycan staining in the sarcolemma in both *Sgcg*^{-/-} and wild-type mice.

Clinically, this finding is critically important. The present data indicate that FTY720 is perhaps curative by re-establishing the DGC, including δ -sarcoglycan, and not just palliative. More work is needed to determine whether DGC restoration also causes reduced fibrosis and functional recovery of FTY720 treatment, and how this restoration is being accomplished by FTY720 treatment.

Early FTY720 treatment also significantly reduced skeletal, cardiac, and diaphragm muscle fibrosis. Reduced fibrosis is evident in the anatomical (Fig. 2) and fibronectin staining (Fig. 5) images. Multiple reports have demonstrated that, in murine and human MD, the diaphragm is especially fibrotic.^{6,26} Also, because of the respiratory failure leading to death of many MD patients, a careful assessment of diaphragm function was conducted. The reduced diaphragm fibrosis was also functionally evident in the plethysmography data, which indicates improved function by early FTY720 treatment (Fig. 6). The directional changes of these characteristics (decreased values) confirm that the functional changes were due to fibrosis. Fibrosis would slow the relaxation stages of respiration, and therefore lead to slower PIF and PEF. Decreased MV and EF₅₀ are also consistent with a fibrotic and therefore stiff diaphragm. Early FTY720 treatment prevented these fibrotic functional changes and restored diaphragm function to be insignificantly different from the wild-type D2 mice. In addition to these 4 important respiratory parameters, FTY720 treatment also restored time of inhalation to near wild-type levels (refer to Table SI in Supplementary Material, available online). The important enhanced pause (penh) parameter was not significantly different between the untreated mutants and the wild-type animals, very likely because the mutants were too young to have progressed to full respiratory pathology.¹

As expected, as previous publications have shown there is not enough cardiac pathology to elicit functional changes at such a young age,¹ no echocardiographic differences were found between any of the groups.

Due to the many sites at which FTY720 decreased pathology, I sketched a working model for the postulated mechanisms for inhibition of LGMD-2C disease progression (Fig. 7). In addition, previous studies have identified that FTY720 and/ or S1P decreases apoptosis,²⁷ increases satellite cell capabilities,^{28,29} and decreases immune infiltration and cytokines.¹¹ Because FTY720 has a long half-life of 6–9 days, has a flat pharmacokinetic concentration profile,^{30,31} and inhibits multiple sites throughout disease progression, I hypothesize that lower doses could be effective in the LGMD-2C mouse model and, ultimately, in patients. This possibility is currently being tested.

Because of the long list of possible FTY720 benefits of muscle regeneration, the field is wide open with regard to the actual molecular mechanisms leading to the results described herein. Based on the work of others, portions of the FTY720 benefits are likely due to immune inhibition¹¹ and reduced fibrosis.¹² Furthermore, as established by the EBD data described here, additional benefits likely arise from increasing skeletal muscle sarcolemmal integrity. Experiments designed to identify which specific mechanisms are involved in this phenotypic reduction are now being conducted. Further experiments are also underway to investigate the mechanisms of DGC re-establishment to the sarcolemma. There are many questions created by this study. Although many experiments have been conducted using S1P and skeletal muscle, the specific effects of FTY720 on muscle cells have yet to be established. In addition, experiments with longer duration prevention and reversal strategies and lower doses are required. Furthermore, specific molecular mechanisms, including immune mechanisms, are currently being investigated.

The mice in these experiments received unphosphorylated FTY720. Future experiments should identify the most effective anti-muscular dystrophy FTY720 format and balance that against possible undesired side effects.³² Both forms of FTY720 have biological activities, and both are intricately controlled and interchanged by cellular mechanisms.¹⁴

Because LGMD-2C is a devastating disease, both progressive and fully lethal, I propose that FTY720 be used as a co-therapy. The goal is to utilize a low FTY720 dose that avoids side effects in patients but will be functional and can enhance the benefits of an additional treatment. Such a strategy has been proposed for many of the MD treatments currently in the pipeline.³³ Because of the re-establishment of DGC members with FTY720 treatment, I envision that this could also be a co-therapy with cell- or gene-based therapies to boost the effectiveness of restoring a functioning DGC.

Acknowledgments

This study was supported by the National Institutes of Health (R01 HL102322 and R21 AR069196 to A.H.).

The author thanks Dr. Jesus Garcia, Dr. R. John Solaro, Dr. Beata M. Wolska, and Jeannine Wilk for invaluable scientific discussions. I also thank Dr. Randall Jaffe for the anatomy images in Figure 2, and Dr. Robert Gaffin for the expert echocardiography and analysis. Some of the data and statistical analyses were performed by Wassim Hassan and Jamal Azhari.

Abbreviations

ANOVA analysis of variance

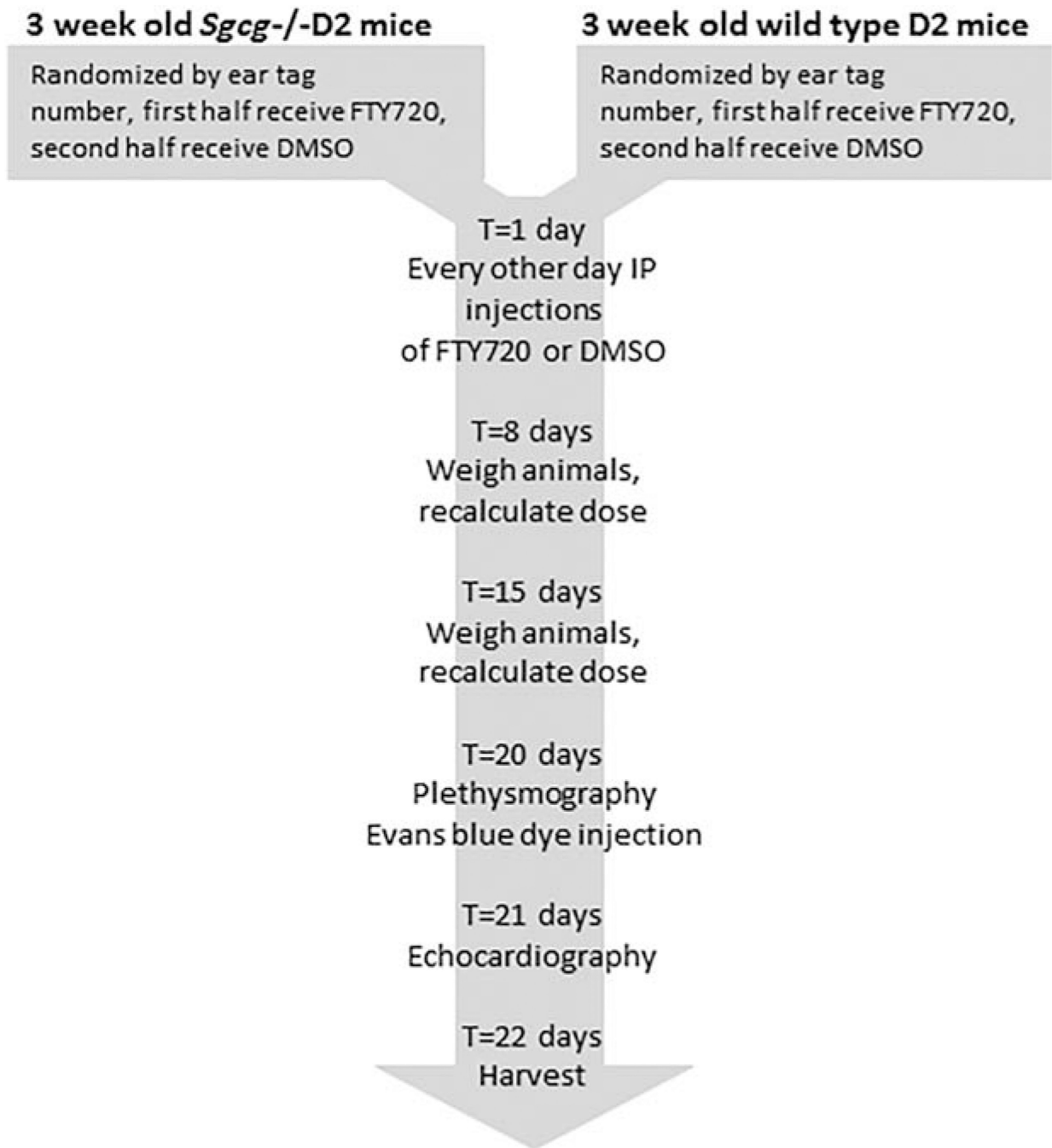
D2	DBA2/J mouse strain
DGC	dystrophin–glycoprotein complex
DMSO	dimethylsulfoxide
EBD	Evans blue dye
ECM	extracellular matrix
ECM	extracellular matrix
EF₅₀	expiratory flow at 50% of tidal volume
Sgcg	γ -sarcoglycan
HOP	hydroxyproline
LGMD	limb-girdle muscular dystrophy
MD	muscular dystrophy
MV	minute volume
PAK1	serine/threonine–protein kinase
PBS	phosphate-buffered saline
PEF	peak expiratory flow
PIF	peak inspiratory flow
S1P	sphingosine-1-phosphate

References

1. Roberts NW, Holley-Cuthrell J, Gonzalez-Vega M, Mull AJ, Heydemann A. Biochemical and Functional comparisons of mdx and Sgcg (–/–) muscular dystrophy mouse models. *Biomed Res Int*. 2015;1314362.
2. Mann CJ, Perdiguero E, Kharraz Y, Aguilar S, Pessina P, Serrano AL, et al. Aberrant repair and fibrosis development in skeletal muscle. *Skelet Muscle*. 2011; 1:21. [PubMed: 21798099]
3. Vorotnikova E, McIntosh D, Dewilde A, Zhang J, Reing JE, Zhang L, et al. Extracellular matrix-derived products modulate endothelial and progenitor cell migration and proliferation in vitro and stimulate regenerative healing in vivo. *Matrix Biol*. 2010; 29:690–700. [PubMed: 20797438]
4. Nigro V, Piluso G. Spectrum of muscular dystrophies associated with sarcolemmal-protein genetic defects. *Biochim Biophys Acta*. 2015; 1852:585–593. [PubMed: 25086336]
5. Hack AA, Ly CT, Jiang F, Clendenin CJ, Sigrist KS, Wollmann RL, et al. Gamma-sarcoglycan deficiency leads to muscle membrane defects and apoptosis independent of dystrophin. *J Cell Biol*. 1998; 142:1279–1287. [PubMed: 9732288]
6. Heydemann A, Huber JM, Demonbreun A, Hadhazy M, McNally EM. Genetic background influences muscular dystrophy. *Neuromuscul Disord*. 2005; 15:601–609. [PubMed: 16084087]
7. Heydemann A, Ceco E, Lim JE, Hadhazy M, Ryder P, Moran JL, et al. Latent TGF-beta-binding protein 4 modifies muscular dystrophy in mice. *J Clin Invest*. 2009; 119:3703–3712. [PubMed: 19884661]

8. Straub V, Bertoli M. Where do we stand in trial readiness for autosomal recessive limb girdle muscular dystrophies? *Neuromuscul Disord.* 2016; 26:111–125. [PubMed: 26810373]
9. Bello L, Gordish-Dressman H, Morgenroth LP, Henricson EK, Duong T, Hoffman EP, et al. Prednisone/prednisolone and deflazacort regimens in the CINRG Duchenne Natural History Study. *Neurology.* 2015; 85:1048–1055. [PubMed: 26311750]
10. Sanford M. Fingolimod: a review of its use in relapsing-remitting multiple sclerosis. *Drugs.* 2014; 74:1411–1433. [PubMed: 25063048]
11. Luo ZJ, Tanaka T, Kimura F, Miyasaka M. Analysis of the mode of action of a novel immunosuppressant FTY720 in mice. *Immunopharmacology.* 1999; 41:199–207. [PubMed: 10428648]
12. Liu W, Zi M, Tsui H, Chowdhury SK, Zeef L, Meng QJ, et al. A novel immunomodulator, FTY-720 reverses existing cardiac hypertrophy and fibrosis from pressure overload by targeting NFAT (nuclear factor of activated T-cells) signaling and periostin. *Circ Heart Fail.* 2013; 6:833–844.
13. Liu W, Zi M, Naumann R, Ulm S, Jin J, Taglieri DM, et al. Pak1 as a novel therapeutic target for antihypertrophic treatment in the heart. *Circulation.* 2011; 124:2702–2715. [PubMed: 22082674]
14. Olivera A, Allende ML, Proia RL. Shaping the landscape: metabolic regulation of S1P gradients. *Biochim Biophys Acta.* 2013; 1831:193–202. [PubMed: 22735358]
15. Nguyen-Tran DH, Hait NC, Sperber H, Qi J, Fischer K, Ieronimakis N, Pantoja M, et al. Molecular mechanism of sphingosine-1-phosphate action in Duchenne muscular dystrophy. *Dis Model Mech.* 2014; 7:41–54. [PubMed: 24077965]
16. Donati C, Cencetti F, Bruni P. New insights into the role of sphingosine 1-phosphate and lysophosphatidic acid in the regulation of skeletal muscle cell biology. *Biochim Biophys Acta.* 2013; 1831:176–184. [PubMed: 22877992]
17. Farini A, Meregalli M, Belicchi M, Battistelli M, Parolini D, D'Antona G, et al. T and B lymphocyte depletion has a marked effect on the fibrosis of dystrophic skeletal muscles in the scid/mdx mouse. *J Pathol.* 2007; 213:229–238. [PubMed: 17668421]
18. Pantoja M, Fischer KA, Ieronimakis N, Reyes M, Ruohola-Baker H. Genetic elevation of sphingosine 1-phosphate suppresses dystrophic muscle phenotypes in *Drosophila*. *Development.* 2013; 140:136–146. [PubMed: 23154413]
19. Ieronimakis N, Pantoja M, Hays AL, Dosey TL, Qi J, Fischer KA, et al. Increased sphingosine-1-phosphate improves muscle regeneration in acutely injured mdx mice. *Skelet Muscle.* 2013; 3:20. [PubMed: 23915702]
20. Schaphorst KL, Chiang E, Jacobs KN, Zaiman A, Natarajan V, Wigley F, et al. Role of sphingosine-1 phosphate in the enhancement of endothelial barrier integrity by platelet-released products. *Am J Physiol Lung Cell Mol Physiol.* 2003; 285:L258–267. [PubMed: 12626332]
21. Matsumura K, Ohlendieck K, Ionasescu W, Tome FM, Nonaka I, Burghes AH, et al. The role of the dystrophin-glycoprotein complex in the molecular pathogenesis of muscular dystrophies. *Neuromuscul Disord.* 1993; 3:533–535. [PubMed: 8186706]
22. Zipf RE, Webber JM, Grove GR. A comparison of routine plasma volume determination methods using radio-iodinated human serum albumin and Evans blue dye (T-1824). *J Lab Clin Med.* 1955; 45:800–805.
23. Matsuda R, Nishikawa A, Tanaka H. Visualization of dystrophic muscle fibers in mdx mouse by vital staining with Evans blue: evidence of apoptosis in dystrophin-deficient muscle. *J Biochem.* 1995; 118:959–964. [PubMed: 8749313]
24. Garcia JG, Liu F, Verin AD, Birukova A, Dechert MA, Gerthoffer WT, et al. Sphingosine 1-phosphate promotes endothelial cell barrier integrity by Edg-dependent cytoskeletal rearrangement. *J Clin Invest.* 2001; 108:689–701. [PubMed: 11544274]
25. Dudek SM, Camp SM, Chiang ET, Singleton PA, Usatyuk PV, Zhao Y, et al. Pulmonary endothelial cell barrier enhancement by FTY720 does not require the S1P1 receptor. *Cell Signal.* 2007; 19:1754–1764. [PubMed: 17475445]
26. Webster C, Silberstein L, Hays AP, Blau HM. Fast muscle fibers are preferentially affected in Duchenne muscular dystrophy. *Cell.* 1988; 52:503–513. [PubMed: 3342447]

27. Suzuki S, Li XK, Shinomiya T, Enosawa S, Kakefuda T, Mitsusada M, et al. Induction of lymphocyte apoptosis and prolongation of allograft survival by FTY720. *Transplant Proc.* 1996; 28:2049–2050. [PubMed: 8769151]
28. Loh KC, Leong WI, Carlson ME, Oskouian B, Kumar A, Fyrst H, et al. Sphingosine-1-phosphate enhances satellite cell activation in dystrophic muscles through a S1PR2/STAT3 signaling pathway. *PLoS One.* 2012; 7:e37218. [PubMed: 22606352]
29. Calise S, Blescia S, Cencetti F, Bernacchioni C, Donati C, Bruni P. Sphingosine 1-phosphate stimulates proliferation and migration of satellite cells: role of SIP receptors. *Biochim Biophys Acta.* 2012; 1823:439–450. [PubMed: 22178384]
30. Kovarik JM, Schmouder RL, Slade AJ. Overview of FTY720 clinical pharmacokinetics and pharmacology. *Ther Drug Monit.* 2004; 26:585–587. [PubMed: 15570180]
31. Kappos L, Radue EW, O'Connor P, Polman C, Hohlfeld R, Calabresi P, et al. A placebo-controlled trial of oral fingolimod in relapsing multiple sclerosis. *N Engl J Med.* 2010; 362:387–401. [PubMed: 20089952]
32. Ntranos A, Hall O, Robinson DP, Grishkan IV, Schott JT, Tosi DM, et al. FTY720 impairs CD8 T-cell function independently of the sphingosine-1-phosphate pathway. *J Neuroimmunol.* 2014; 270:13–21. [PubMed: 24680062]
33. Griggs RC, Herr BE, Reha A, Elfring G, Atkinson L, Cwik V, et al. Corticosteroids in Duchenne muscular dystrophy: major variations in practice. *Muscle Nerve.* 2013; 48:27–31. [PubMed: 23483575]

**FIGURE 1.**

Schematic of the animal protocol. Mutant (top left) or wild-type (top right) DBA2/J (D2) mice were randomly assigned to FTY720 or DMSO groups. The 4 groups were treated identically throughout the 3-week protocol. The mice received intraperitoneal injection every other day. Every Monday the mice were weighed, and the therapeutic or vehicle doses were recalculated. Two days before harvest the respiratory function of all mice was assessed by whole-body plethysmography, and the mice received an intraperitoneal dose of Evans blue dye. One day before harvest, the mice were anesthetized for echocardiography.

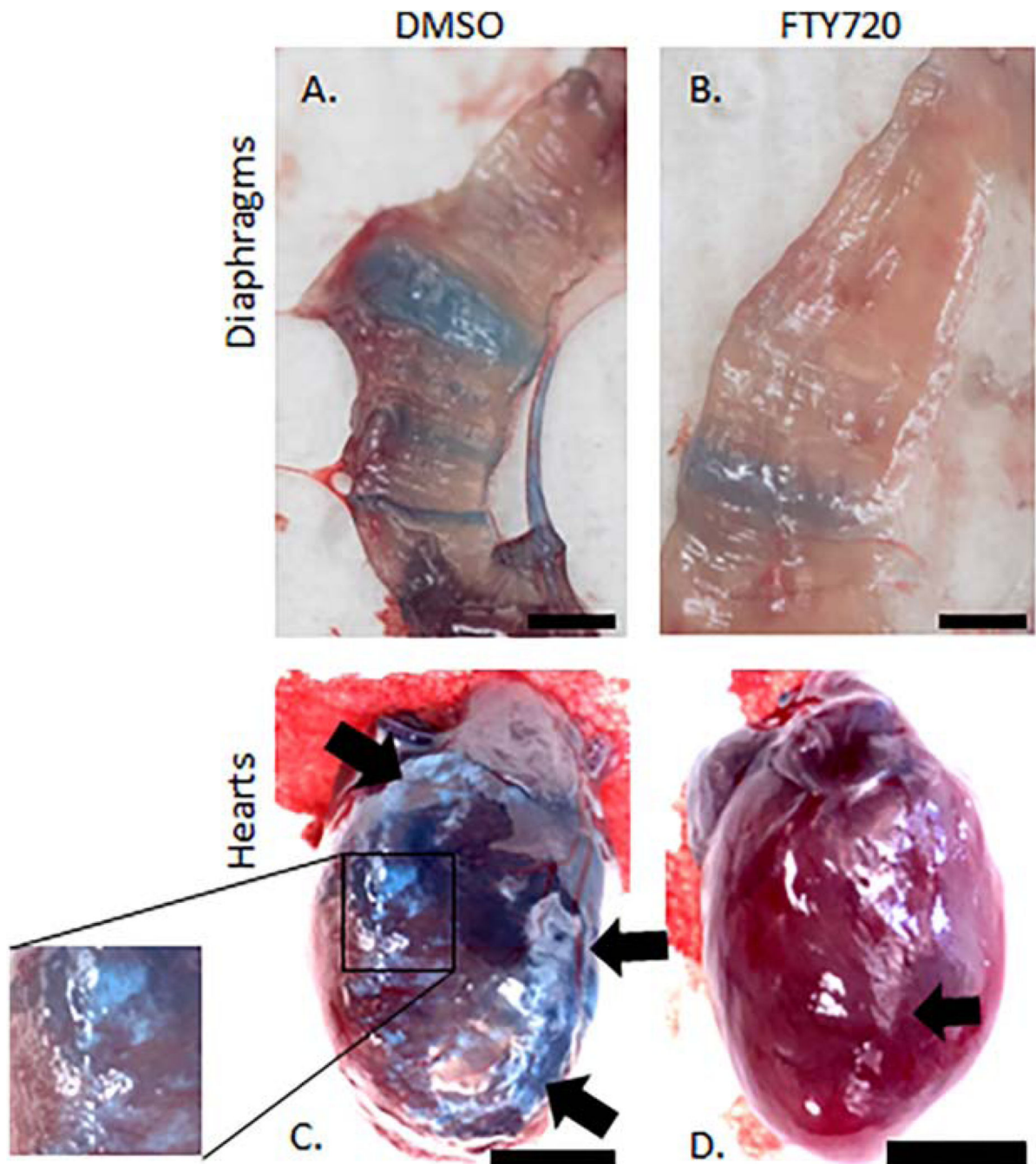
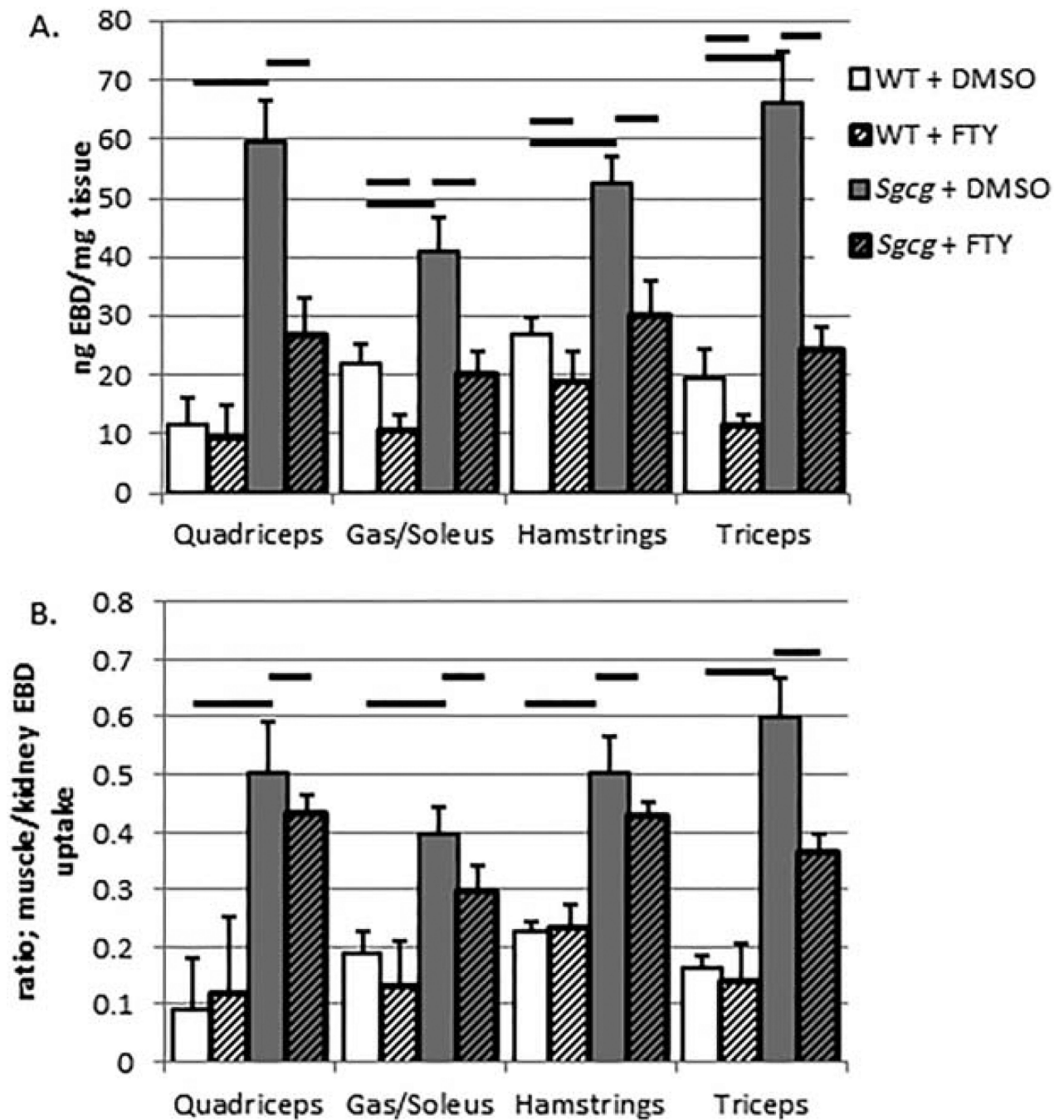


FIGURE 2. Representative anatomy images demonstrate reduced EBD uptake and fibrosis after FTY720 treatment. The FTY720-treated diaphragm (**B**) contained less EBD and fewer fibrotic fibers than the control diaphragm (**A**). The control heart (**C**) displayed extensive fibrosis throughout the right ventricle (delineated by arrows, and focused upon in the inset). The treated heart (**D**) had smaller regions of fibrosis (indicated by an arrow) at the edges of the right ventricle. Black bars: 3 mm.

**FIGURE 3.**

FTY720 treatment decreased skeletal muscle EBD uptake. Total EBD uptake was reduced in both wild-type and *Sgcg* mutant animals by FTY720 treatment (A) (averages and standard errors). After correcting for FTY720-reduced endothelial cell permeability by normalizing to kidney EBD uptake, the treated *Sgcg* animals had significantly less EBD uptake (B). WT + DMSO, $N = 5$; WT+FTY, $N = 5$; *Sgcg*+DMSO, $N = 11$; *Sgcg*+FTY, $N = 14$. Thick black bars indicate ANOVA, $P < 0.05$.

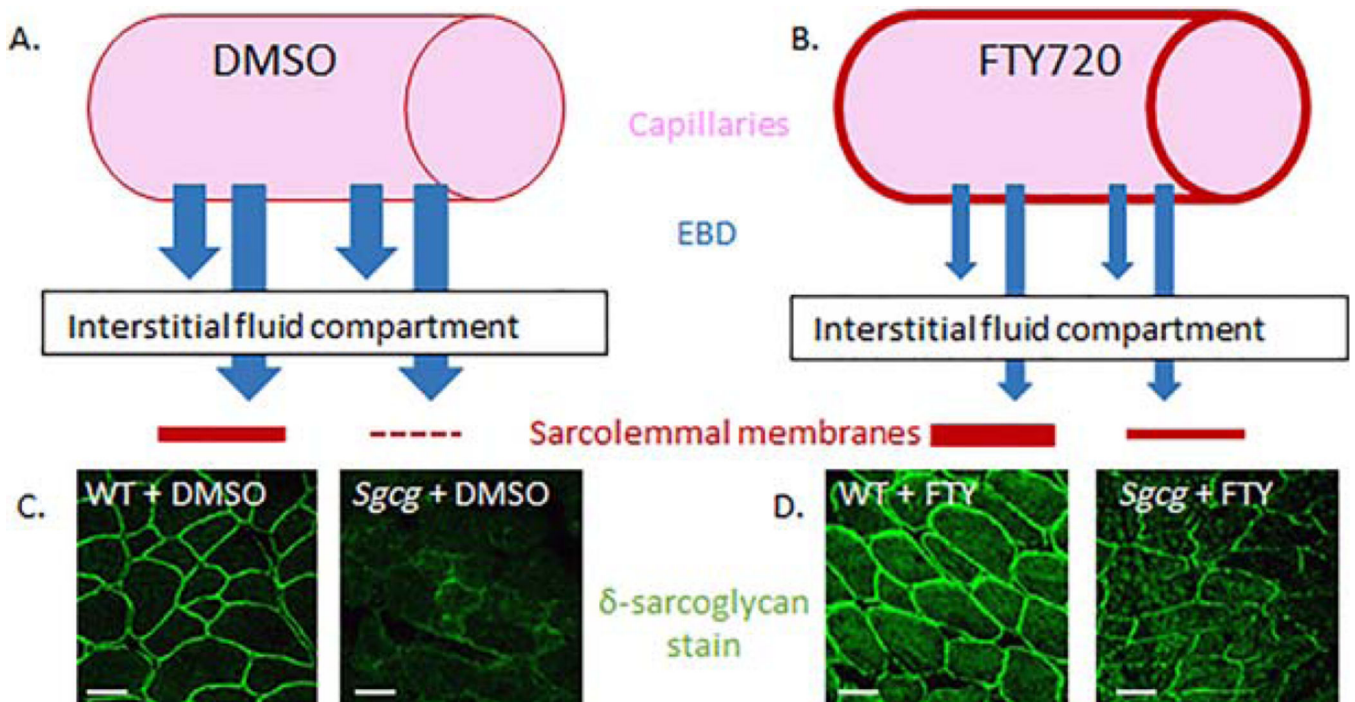
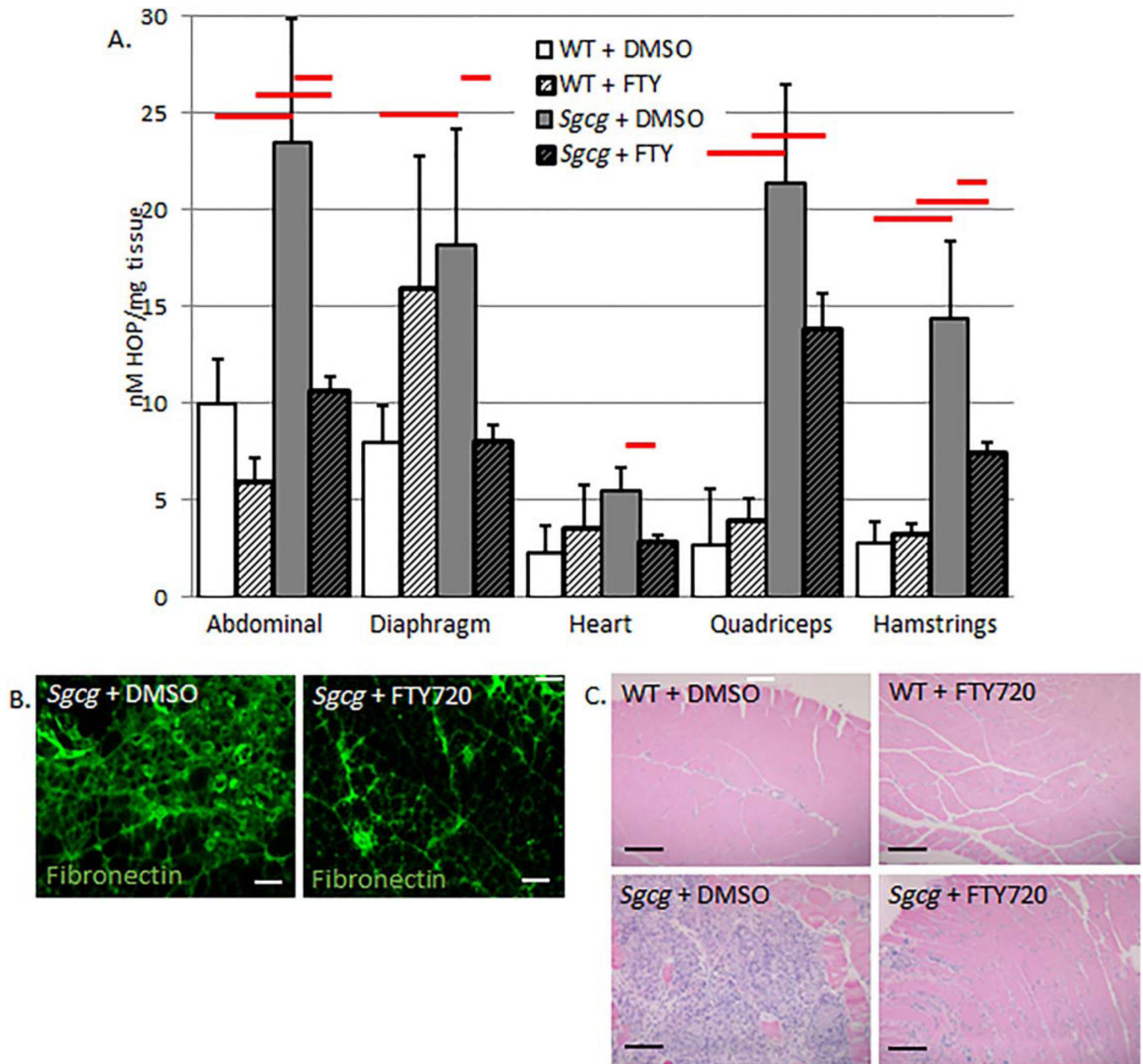
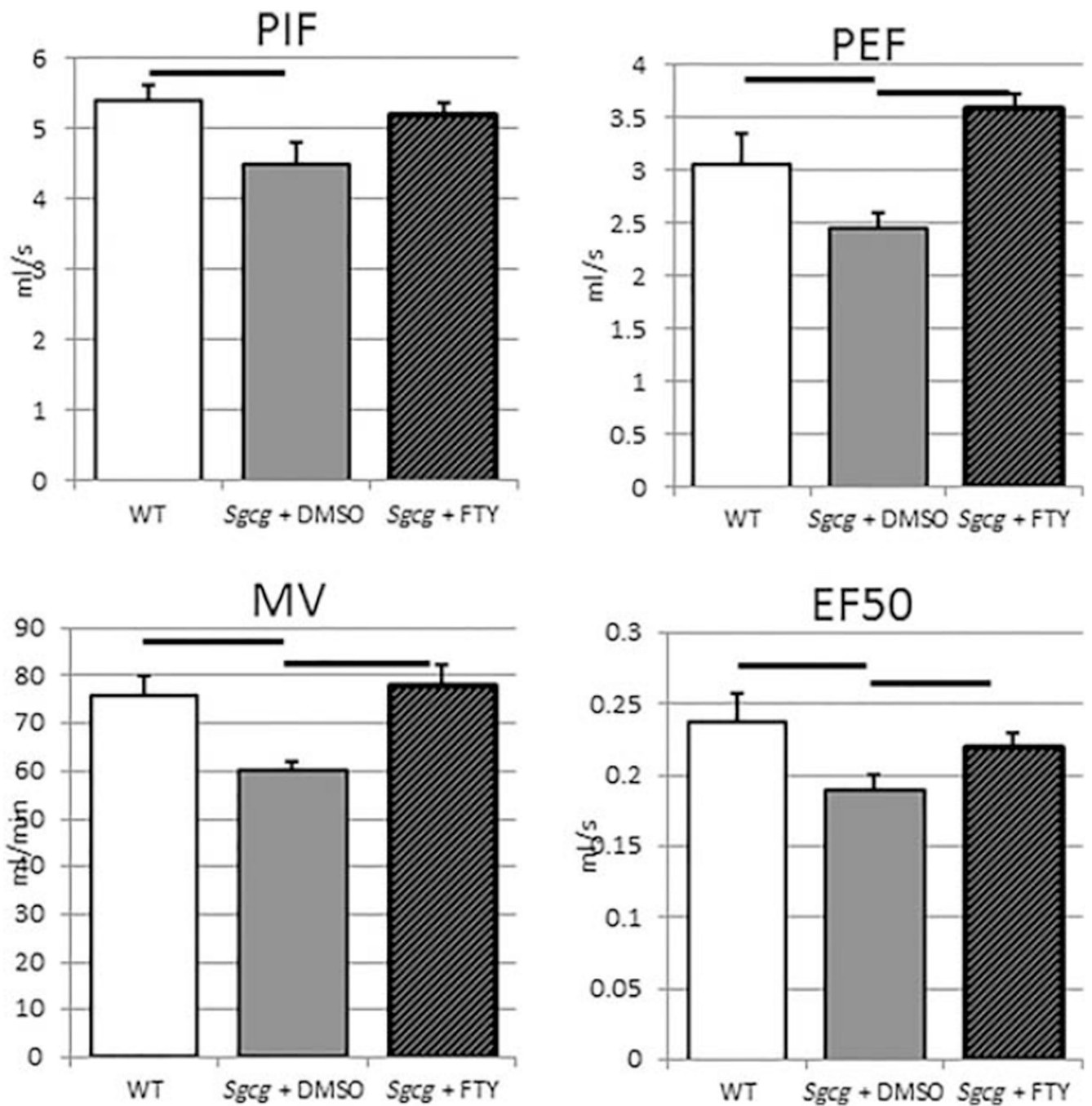


FIGURE 4.

A working model of FTY720's effects on endothelial cells and skeletal muscle sarcolemma. Compared with control DMSO-treated endothelium (A), FTY720 reduced endothelial cell permeability (B). FTY720 also reinforced the sarcolemmal membranes (D) compared with the control DMSO-treated muscle cells (C). δ -Sarcoglycan staining of wild-type and *Sgcg* mutant quadriceps (C, D). For (C) and (D), images were taken at 20 \times original magnification with identical microscope settings. Bars: 50 μ m.

**FIGURE 5.**

FTY720 quantitatively reduces hydroxyproline content in skeletal, cardiac, and diaphragm muscle groups from muscular dystrophy mice (A). Decreased fibronectin staining in FTY720-treated quadriceps (B). Masson trichrome staining also demonstrated reduced fibrosis and immune infiltrate after FTY720 treatment (C). (A) WT+DMSO, $N=5$; WT+FTY, $N=6$; *Sgcg*+DMSO, $N=11$; *Sgcg*+FTY, $N=16$. Red bars indicate ANOVA, $P < 0.05$. Images were taken at 20 \times (B) (bars: 200 μ m) and 4 \times (C) (bars: 200 μ m), with identical microscope settings for each group.

**FIGURE 6.**

Decreased muscular dystrophy respiratory dysfunction after 3 weeks of FTY720 treatment. PIF, peak inspiratory flow; PEF, peak expiratory flow; MV, minute volume; EF50 expiratory flow at 50% of tidal volume. WT+DMSO, $N = 4$; Sgcg+DMSO, $N = 8$; Sgcg+FTY, $N = 8$. Bars represent ANOVA, $P < 0.05$.

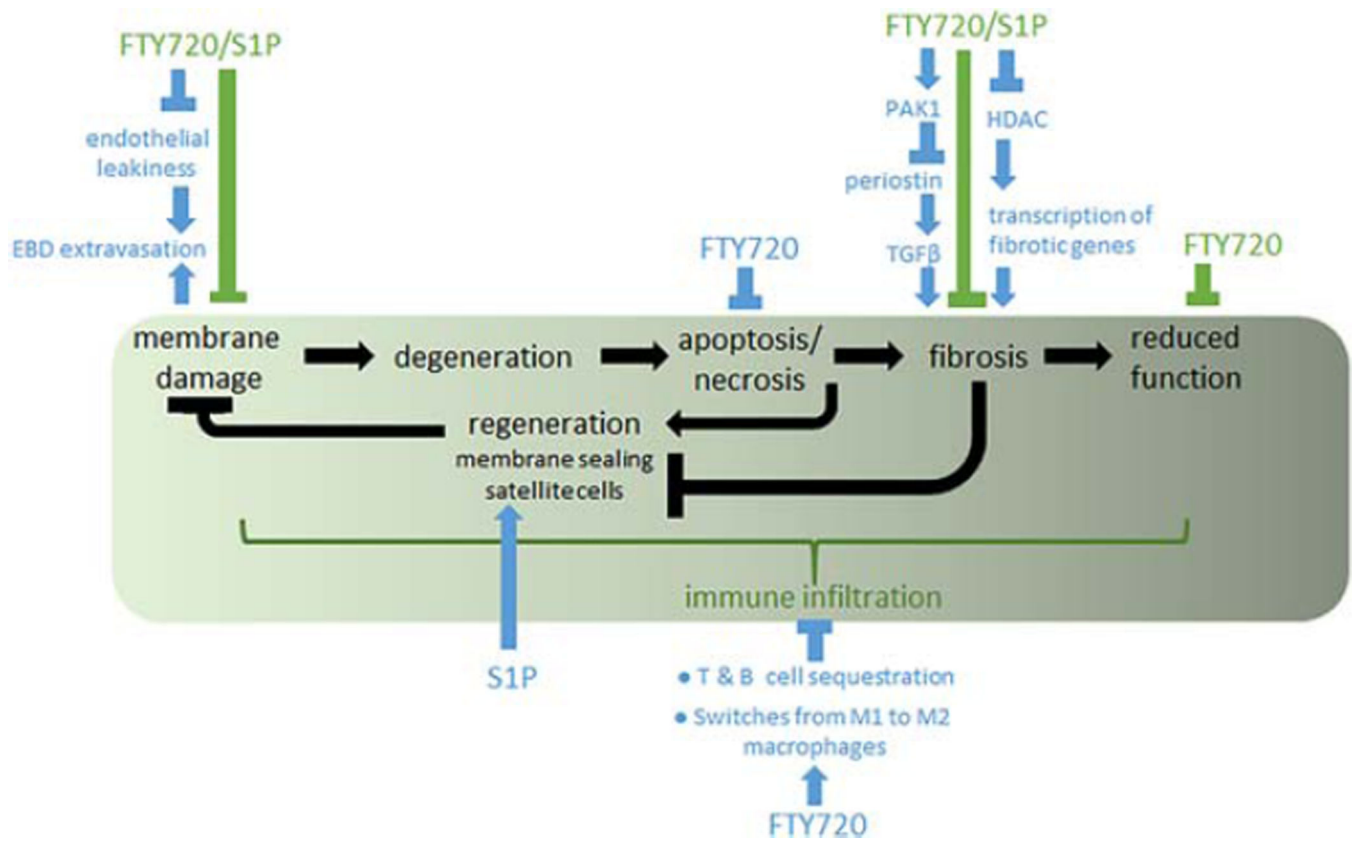


FIGURE 7.

Current working model of the multiple benefits of FTY720 treatment on LGMD-2C. The green box indicates LGMD-2C disease progression, becoming worse as the patient and mouse progress along the sequence from left to right. FTY720 and/or S1P have been found to beneficially affect multiple points along the progression. Data identified or affirmed in this study are indicated with green bars. Data from previous publications are indicated with blue bars and arrows, and are referenced in the text.

Table 1

Statistical data from the Evans blue dye and hydroxyproline graphs

EBD	Abdominals	Quadriceps	Gas/Sol	Hamstrings	Triceps
WT+DMSO					
Average	63.87	11.80	22.14	26.79	19.53
Standard error	7.69	4.46	3.18	3.02	4.72
<i>N</i>	5	5	5	5	5
WT+FTY720					
Average	48.78	9.41	10.69	18.98	11.54
SE	7.73	5.59	2.63	4.87	1.60
<i>N</i>	5	5	5	5	5
<i>S</i> _{EG} +DMSO					
Average	65.31	59.50	41.05	52.65	66.30
Standard error	8.16	6.97	5.55	4.53	8.71
<i>N</i>	8	8	8	8	8
<i>S</i> _{EG} +FTY720					
Average	38.81	26.77	20.20	30.31	24.47
Standard error	5.77	6.33	3.81	5.66	3.78
<i>N</i>	13	12	13	13	13
ANOVA <i>P</i> -value	0.001	0.001	0.005	0.022	0
EBD normalized to kidney values					
Abdominals					
Quadriceps					
Gas/Sol					
Hamstrings					
Triceps					
WT+DMSO					
Average	0.5516	0.0931	0.1870	0.2248	0.1632
Standard error	0.0878	0.0400	0.0182	0.0215	0.0424
<i>N</i>	5	5	5	5	5
WT+FTY720					
Average	0.6130	0.1190	0.1317	0.2342	0.1407
Standard error	0.1324	0.0784	0.0381	0.0655	0.0209
<i>N</i>	5	5	5	5	5
<i>S</i> _{EG} +DMSO					

EBD	Abdominals	Quadriceps	Gas/Sol	Hamstrings	Triceps
Average	0.7366	0.5019	0.3973	0.5039	0.6016
Standard error	0.0882	0.0472	0.0637	0.0669	0.0626
<i>N</i>	8	8	8	8	8
<i>Sgcg+FTY720</i>					
Average	0.5726	0.4352	0.2957	0.4270	0.3638
Standard error	0.0305	0.0446	0.0255	0.0332	0.0304
<i>N</i>	13	12	13	13	13
ANOVA <i>P</i> -value	0.363	0	0.009	0.008	0
HOP					
Abdominals					
Diaphragm					
Heart					
Quadriceps					
Hamstrings					
WT+DMSO					
Average	9.90	7.91	2.29	2.67	2.72
Standard error	2.32	1.93	1.36	2.88	1.15
<i>N</i>	5	5	5	5	5
WT+FTY720					
Average	5.90	15.85	3.49	3.84	3.23
Standard error	1.22	4.98	2.24	1.18	0.53
<i>N</i>	6	6	6	6	6
Sgcg+DMSO					
Average	23.48	18.11	5.46	21.31	14.36
Standard error	6.32	4.46	1.14	5.11	3.94
<i>N</i>	9	9	9	9	9
Sgcg+FTY720					
Average	10.57	7.97	2.76	13.82	7.41
Standard error	0.81	0.84	0.40	1.80	0.52
<i>N</i>	14	14	14	14	14
ANOVA <i>P</i> -value	0.006	0.04	0.019	0.006	0.013

Gas, gastrocnemius; Sol, soleus; WT, wild-type. See text for other abbreviations.